RESEARCH ARTICLE

# Optimization of laser cladding process for additive repair of high temperature and high pressure valve sealing surface

**Lei Che[1, 2], Wenlei Sun[1*], Guan Zhang[1, 3], Jiaxin Han[1]**

[1] School of Mechanical Engineering, Xinjiang University, Urumqi, Xinjiang, 830047, China

[2] Xinjiang Uygur Autonomous Region Research Institute of Measurement & Testing, Urumqi, Xinjiang, 830011, China

[3] Engineering Training Center, Xinjiang University, Urumqi, Xinjiang, 830047, China

***Abstract:*** Laser cladding technology is highly suitable for the remanufacturing of thin-walled and easily deformable parts due to its concentrated energy density. Due to the high temperature and high pressure corrosion environment, the valve sealing surface is prone to corrosion, wear and other failures. A nickel-based tungsten carbide alloy layer was prepared on the valve sealing surface substrate material by laser cladding process. By designing orthogonal experiments, the effects of laser power (P), scanning speed (Vb), powder feeding rate (Vf), and WC content (wt%) on the alloy layer were investigated. A fuzzy comprehensive evaluation method including macroscopic quality, microstructure, microhardness, anti-wear performance, oxidation resistance, compactness and corrosion resistance was proposed. The experimental results showed that the hardness, oxidation resistance and corrosion resistance of the laser alloy layer are significantly improved compared with the matrix; the optimum process parameters and the addition ratio of WC powder are laser power (P) of 1.1 kW and scanning speed (Vb) of 800 mm/min. The powder feeding rate (Vf) was 20%, and the WC content was 20% by weight.

***Keywords:*** laser cladding; high temperature and high pressure; process optimization; valve sealing surface; fuzzy comprehensive evaluation

## 1. Introduction

Valves are very important components in petrochemical piping systems [1-5]. The sealing surface of the valve refers to the place where the valve seat and the opening and closing members contact each other. The sealing surface of the valve works in high temperature and high pressure environment, and is subject to wear and corrosion of different media for a long time, and the working conditions are poor, which is easy to cause failure. As the most widely used and most important branch in remanufacturing repair engineering, laser cladding technology has significant advantages. The laser cladding technology can be used to repair the valve, thereby effectively inhibit corrosion and wear, which will inevitably reduce or recover. The loss of the valve promotes the development of the use of valves in various fields.

The quality and performance of laser cladding repairs are highly dependent on the laser cladding process parameters. The laser cladding process parameters mainly include laser power, spot diameter or area, defocus amount, powder feeding speed, scanning speed, and preheating temperature. These parameters vary depending on the material system of the cladding layer and the performance requirements of the cladding layer. At present, researchers have done a lot of research work on the process parameters of laser cladding repair. Tabemero I., Lamikiz A. *et al.* [6] carried out a laser cladding technique to repair the GGG70L material failure stamping die, and proposed the method of melting the AISI 316L on the base DINC45 steel to obtain the best process parameters. Dubourg L., St. Georges L. [7] investigated the process parameters, morphology and surface composition of the cladding layer using specific laser cladding test. The relationship between the process parameters and the characteristics of the cladding layer of laser cladding on the


doi: 10.18063/msmr.v2i2.932

surface of low carbon steel was obtained. Ge Jiangbo, Zhang Anfeng *et al*. [8] studied the relationship between the height, width and forming quality of the cladding layer obtained by using different process parameters in the LMDF test of DZ125L alloy parts, and analyzed the relationship between the parameters. Xiong *et al*. [9] used a synchronous laser cladding technique on the surface of Q235 steel to coat Ni60 and Ni60 alloy powders containing 25% WC. The WC grain distribution of the Ni60 alloy cladding layer containing 25% WC ratio is uniform, and the wear resistance and microhardness are improved compared with Ni60 powder. Although the researchers have conducted various studies on the optimization of laser cladding process parameters and obtained many significant research results, there are still very few reports on laser cladding repair of failed parts under high temperature and high pressure conditions.

In this paper, multiple sets of cladding layers can be obtained by adding different amounts of WC particles to the Co-based powder as the reinforcing phase [10], while changing the process parameters. The obtained cladding layer was subjected to macroscopic surface forming observation, and after 600 ℃ and 100 MPa high temperature and high pressure treatment for 2 h, the interface characteristics of the micro-cladding layer and the substrate were observed, as well as corrosion resistance, wear resistance and compactness. The three aspects of the test were carried out. The fuzzy technology under the improved European metric weight coefficient and the classical comprehensive evaluation theory were used to comprehensively evaluate the performance of the laser cladding layer, and the optimal process parameters for the repair of the valve sealing surface under high temperature and high pressure were obtained. Addition ratio with WC powder.

# 2. Research on laser cladding technology of valve sealing surface

## 2.1 Test materials and methods

### 2.1.1 Test matrix material

The test uses 1Cr18Ni9Ti stainless steel with the same material as the valve sealing surface as the base body, and the size is 110 mm × 60 mm × 6 mm. Its chemical composition is shown in Table 1.

| C | Si | Mn | S | P | Cr | Ni | Ti |
|---|---|---|---|---|---|---|---|
| 0.08 | 1.00 | 2.00 | 0.030 | 0.045 | 18.00 | 9.00 | 0.60 |

Table 1. Chemical composition of base material (wt%)

### 2.1.2 Selection of cladding materials

A mixed powder of a Co-based alloy powder and a WC hard powder is used as a cladding material. The composition of the Co-based alloy powder material is shown in Table 2. The WC powder added as the reinforcing phase is a cast hardness ceramic particle, and the chemical composition is shown in Table 3.

| C | Cr | Si | W | Fe | Mo | Ni | Mn | Co |
|---|---|---|---|---|---|---|---|---|
| 1.60 | 28.00 | 1.15 | 4.50 | 0.50 | 1.00 | 3.00 | 1.00 | - |

Table 2. Chemical composition of Co-based self-fluxing alloy powder (wt%)

| WC | Total Carbon | Free carbon | Al | Fe | Mg | Si | O |
|---|---|---|---|---|---|---|---|
| ≥99.7 | 5.98 | ≤0.03 | ≤0.002 | ≤0.03 | ≤0.03 | ≤0.03 | ≤0.06 |

Table 3. Chemical composition (wt%) of test WC powder

### 2.1.3 Test method

The test equipment used laser processing system of 4kW fiber laser produced by IPG Company of USA and

cross-flow gas continuous $CO_2$ laser processing system. Before the laser processing, the surface of the 1Cr18Ni9Ti stainless steel substrate was uniformly ground with 80# metallographic sandpaper to remove oxides, oil and other impurities on the surface, and washed with acetone, dried naturally, and used. In order to reduce the evaporation and oxidation of the surface material during the treatment, the molten pool is protected by argon gas, the overlap between the scanning channels is 30%, and the working distance of the nozzle is 22 mm.

The test has four factors and three levels for the three process parameters [laser power (P), scanning speed (Vb) and powder feeding rate (Vf)] that affect the performance of the powder-feeding laser cladding cladding layer, and the WC content (wt%). The L9 (34) orthogonal table with a number of nines. The factors for adjusting the orthogonal test and the level values of the respective parameters are shown in Table 4.

| Test number | Factors and levels | | | |
|---|---|---|---|---|
| | Power P (kW) | Scanning speed $V_b$ (mm/min) | Powder feeding rate Vf (%) | WC content (wt%) |
| 1 | 0.8 | 400 | 20 | 0 |
| 2 | 0.8 | 600 | 30 | 20 |
| 3 | 0.8 | 600 | 40 | 40 |
| 4 | 1.1 | 400 | 30 | 40 |
| 5 | 1.1 | 600 | 40 | 0 |
| 6 | 1.1 | 800 | 20 | 20 |
| 7 | 1.4 | 400 | 40 | 20 |
| 8 | 1.4 | 600 | 20 | 40 |
| 9 | 1.4 | 800 | 30 | 0 |

Table 4. Factors and level test table for laser cladding of 1Cr18Ni9Ti stainless steel

## 2.2 Surface quality and analysis of cladding layer

### 2.2.1 Macro aspects

After the laser cladding is completed, the macroscopic appearance of the surface quality of the test piece obtained by different process parameters is shown in **Figure 1.**

Macroscopic observation shows no surface cracks and pore defects in the above nine samples. It shows the range of the selected process parameters has a relatively good matching with the substrate. From the point of view of good formability of the cladding layer, the reason for the analysis is mainly due to the relatively small alloy content of the Co-based powder, the easy wetting with the base 1Cr18Ni9Ti stainless steel, the sufficient reaction of the molten pool and the high fluidity. Therefore, the appearance formability is good. Since the gas generated in the molten pool reaction is small, it is difficult to aggregate and blast at the surface layer, so the surface is substantially free from splashing.

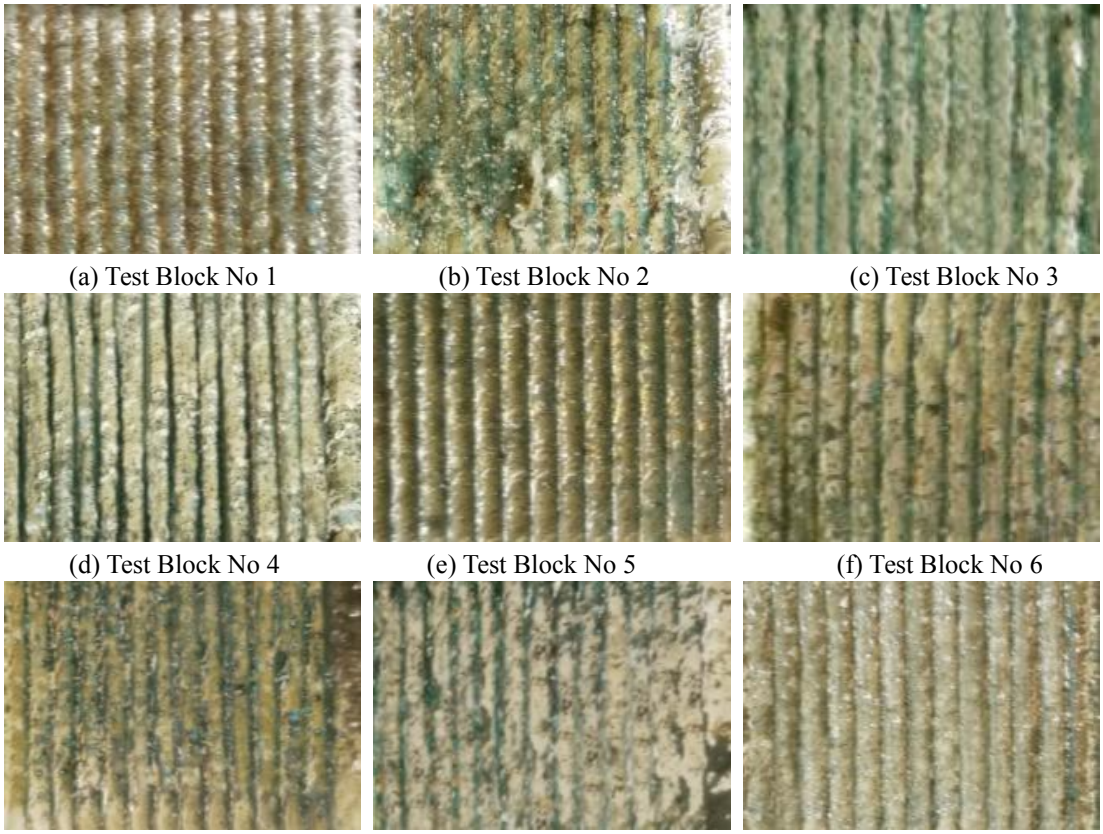

(a) Test Block No 1 (b) Test Block No 2 (c) Test Block No 3

(d) Test Block No 4 (e) Test Block No 5 (f) Test Block No 6

(g) Test Block No 7 (h) Test Block No 8 (i) Test Block No 9

**Figure 1.** The surface quality of the test piece under different laser cladding process parameters

### 2.2.2 Micro aspects

After each test block was subjected to high temperature and high pressure treatment, it was smoothed with sandpaper, and placed under a scanning electron microscope to enlarge it to 2000 times. The interface characteristics are as shown in **Figure 2.**

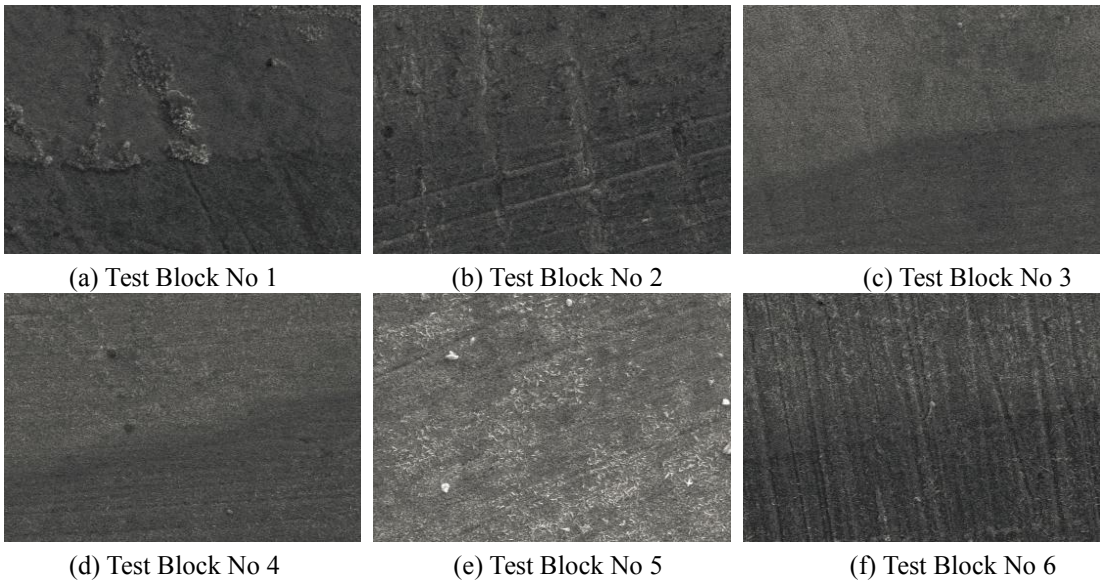

(a) Test Block No 1 (b) Test Block No 2 (c) Test Block No 3

(d) Test Block No 4 (e) Test Block No 5 (f) Test Block No 6

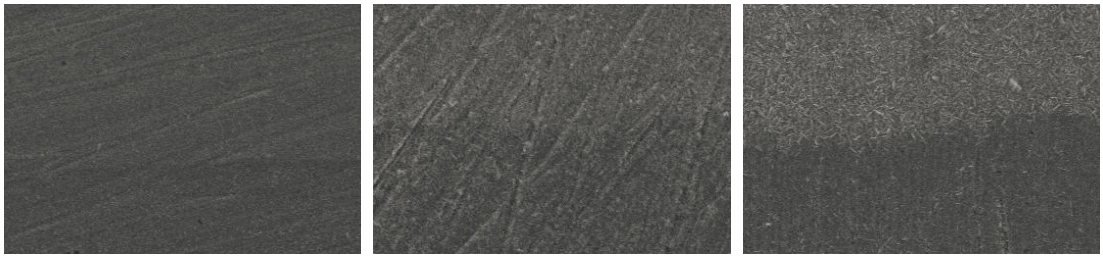

(g) Test Block No 7 (h) Test Block No 8 (i) Test Block No 9

**Figure 2.** 2000x scanning electron microscope interface characteristics of test blocks under different laser cladding process parameters

It can be seen from **Figure 2** that cracks and pores are formed between the cladding layer and the matrix of all the test pieces, and the combination is good. For the test piece containing WC particles, the WC distribution was relatively uniform, and there was no obvious phenomenon of sinking at the bottom. After laser beam heating treatment, the WC particles still maintain their original spherical appearance, only a slight dissolution at the edges, and the surface of the WC particles and the Co-based alloy are also metallurgical bonding.

## 2.3 Microhardness of the cladding layer

The samples obtained by different laser cladding process parameters were subjected to wire cutting, grinding and polishing to prepare microhardness test pieces. The test piece was placed in a dry box, and the temperature was raised to 100 ℃, and the temperature was kept at 1 h to remove moisture. The dried test block is placed in a high-temperature muffle furnace, heated to 500℃, constant temperature for 1 h, and the temperature is lowered to room temperature, and placed in a high-temperature muffle furnace, heated to 600℃, constant temperature for 2 h, and the temperature is lowered to room temperature. The sandpaper was sanded and leveled, and the microhardness value of the cross section of the microhardness sample was tested by a digital microhardness tester. The test load was 500 g and the loading time was 10 s. The obtained data is shown in **Figure 3.**

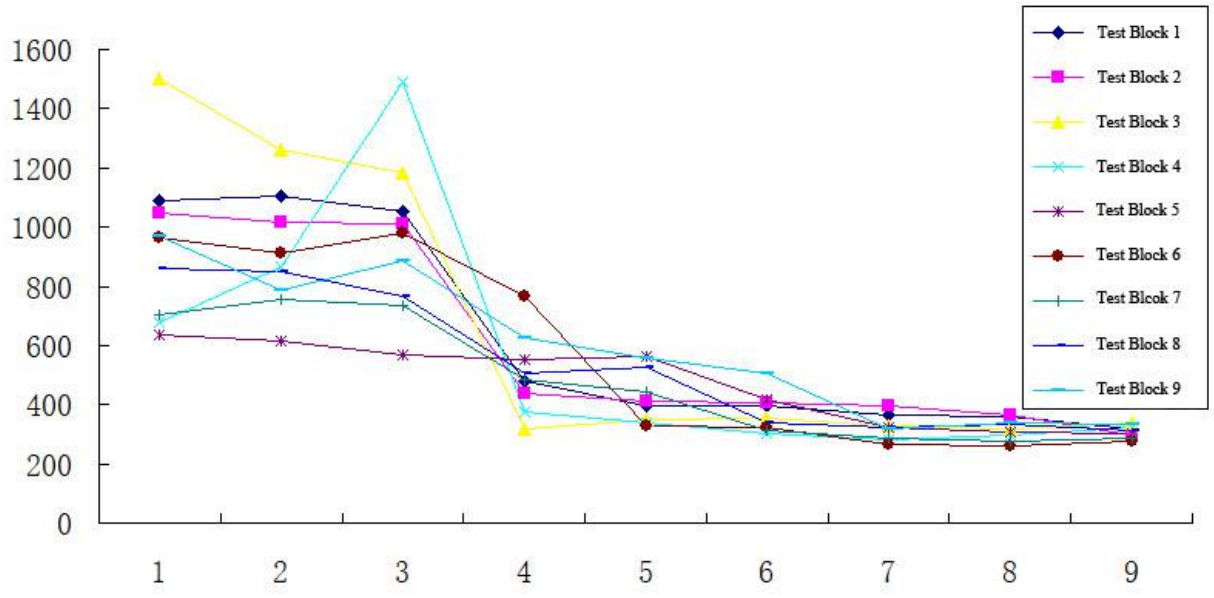


**Figure 3.** Microhardness of different laser cladding process parameters for high temperature processing

It can be found from **Figure 3** that the hardness of the 1Cr18Ni9Ti stainless steel substrate is about 300 HV, and the hardness of the cladding layer obtained by any process parameter cladding is significantly higher than the hardness value of the substrate. The hardness of the Co-based alloy cladding layer is between 800 HV and 1200 HV. For the test pieces containing different content of WC particles, the distribution of hardness along the depth direction is more obvious, especially the test pieces No. 3 and No. 4, the hardness is up to 1498.4HV and 1489.4HV. The reason for this is

that the added WC particles form a hard-line hexagonal hard phase W2C harder than WC under the action of a high-energy laser beam, and WC and W2C form a surrounding phase with Co and Fe. The eutectic carbides Co3W3C and Fe3W3C have very high hardness.

## 2.4 Anti-wear performance

The test for wear resistance was determined by the coefficient of dry friction with the glass. The coefficient of friction is one of the important indicators for measuring the friction properties of materials. Under the same conditions, for the same friction pair, the smaller the friction coefficient, the better the wear resistance; conversely, the worse the wear resistance [12-13]. The dry friction coefficient between each test piece and the glass obtained by the test and calculation is shown in a histogram as shown in **Figure 4.**

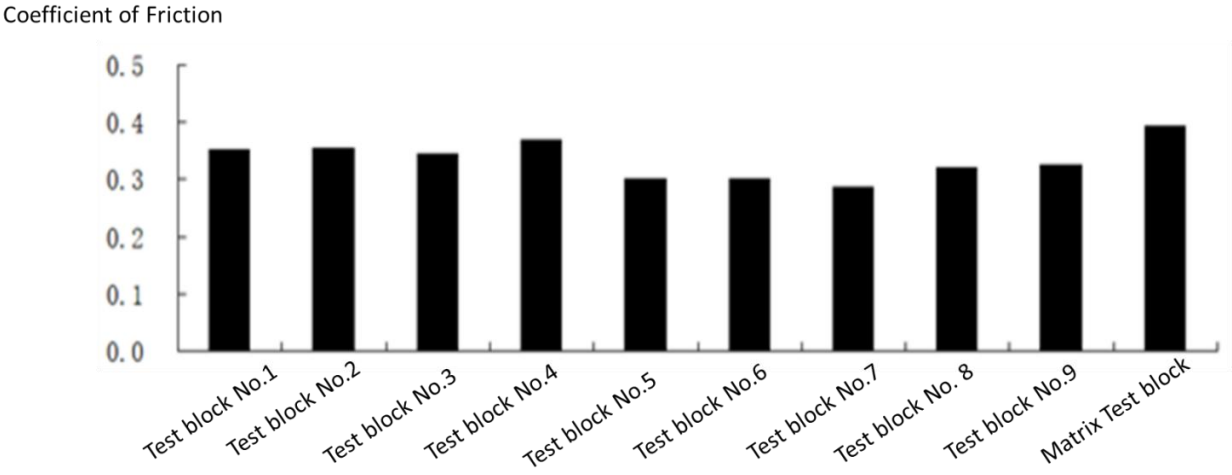


**Figure 4.** Bar graph of dry friction coefficient between each test piece and glass

It can be seen from **Figure 4** that after laser cladding of the 1Cr18Ni9Ti stainless steel material, the friction coefficient of the cladding layer is significantly reduced compared with the substrate, indicating that the wear resistance of the cladding layer is greatly improved relative to the substrate. This is because the Co-based has a very high wear resistance, and the Cr and Mn in the cladding layer also have high wear resistance, and the addition of the WC particles also effectively improves the resistance of the Co-based cladding layer.

## 2.5 Antioxidant properties

The oxidation resistance of equipment working under high temperature and high pressure directly affects the life of equipment and the safety of personnel. The high temperature oxidation performance test was performed on the test piece with the cladding layer and the base test piece. The oxidation test is carried out in a muffle furnace. After the oxidation temperature is raised to 600 ℃, the high temperature is maintained for 2 hours, and the mass before and after oxidation of the test block is weighed by a high-accuracy electronic analytical balance, and the electronic analytical balance is displayed. Can be accurate to 0.001mg. Finally, according to the change of mass before and after oxidation of the test piece and the surface area A, the oxidation increase per unit surface area ( $\Delta m_i$ ) can be calculated:

$$\Delta m_i = \frac{\Delta M_i - \frac{\Delta M_{\text{matrix}}}{A_{\text{J matrix}}} \times A_{\text{J}i}}{A_{\text{R}i}} \quad (1)$$

Where $\Delta M_{\text{matrix}}$ : is the oxidation weight gain of the matrix test block, mg/mm$^2$; $\Delta M_i$ is the oxidation weight

gain of the test block of i, mg/mm$^2$; $A_{Ji}$ is the surface area of the base test piece, mm$^2$; the surface area of the same base material of the test block of i, mm2; $A_{Ri}$ is the surface area of the material of the cladding layer of the test block of i, mm$^2$; $\frac{\Delta M_{matrix}}{A_{Jmatrix}}$ is the oxidation weight gain per unit area of the matrix test block, mg/mm$^2$; $\Delta m_i$ the oxidation weight gain per unit area of the cladding material of the i test block, mg/mm$^2$.

The calculated weight gain per square millimeter of each block of high temperature oxidation is shown in a histogram as shown in **Figure 5**

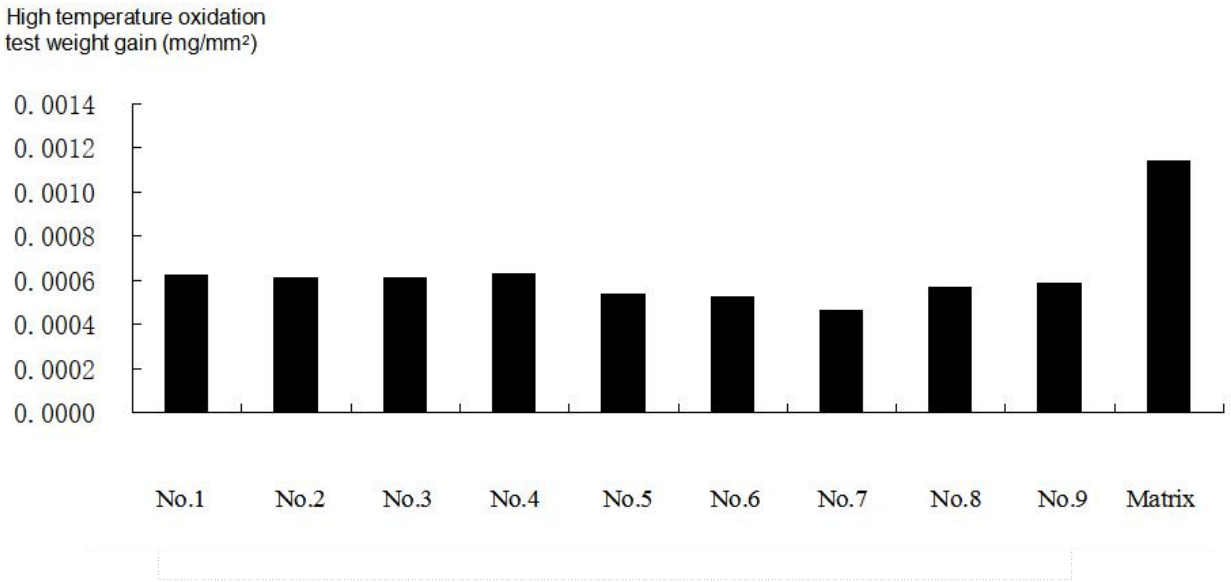


**Figure 5.** Weighted histogram of each test piece per square millimeter of high temperature oxidation

After laser cladding of 1Cr18Ni9Ti stainless steel material, the high-temperature oxidation resistance of the cladding layer is significantly improved compared with the matrix. This is because under the oxidizing conditions, the cladding material is caused to form a thin and closely adhered oxide film on the surface, which can prevent further oxidation of the material, and at the same time, Cr in the cladding layer also has extremely high oxidation resistance.

## 2.6 Density test

The tightness test was performed by two tests of water immersion and oil immersion. The coated sample lines obtained under different laser cladding process parameters are cut into small pieces, and the length, width and height of each test piece are respectively measured, and then the cut test pieces are cleaned by an ultrasonic cleaner and placed in a dry box. The temperature is raised to 100 ℃ for one hour to evaporate the water contained in each test block. After high temperature and high pressure treatment, each test piece is weighed, and then quickly placed in a brown vial containing a high purity water and placed. After 288h30min, take it out and wipe it with a high-grade dry paper towel that does not leave slag, then weigh the test pieces and record. The weight gain per square millimeter of each test piece of the calculated compactness (water immersion test) is shown in a histogram as shown in **Figure 6.**

Similarly, after each test block was treated at high temperature and high pressure, it was placed in a brown vial containing a first standard viscosity oil, placed for 193 h for 35 min, and then taken out, wiped clean, and the mass of each test piece was weighed. The weight gain per square millimeter of each test piece obtained in the compactness (oil immersion test) is shown in a histogram as shown in **Figure 7.**

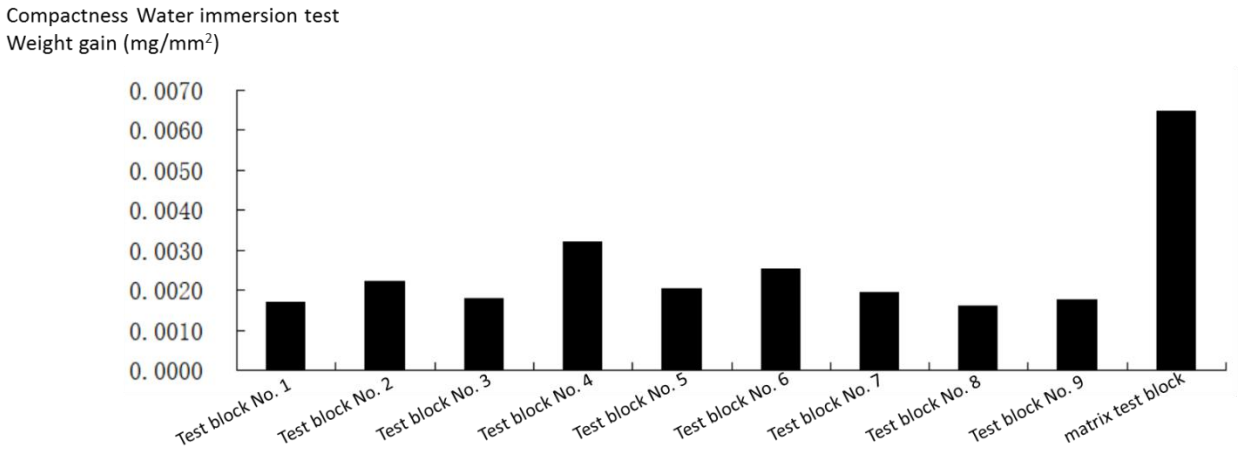


**Figure 6.** Weighted histogram of each test piece per square millimeter of compactness water immersion

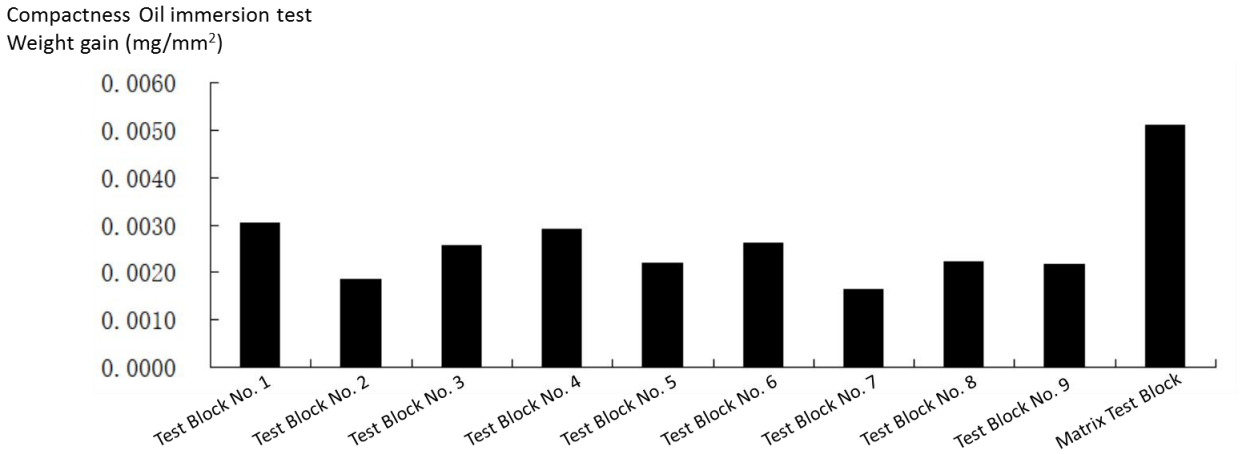


**Figure 7.** Weighted histogram of each test piece per square millimeter of compactness oil immersion

It can be seen from **Figure 6** and **Figure 7** that after laser cladding of the 1Cr18Ni9Ti stainless steel material, the compactness of the cladding layer is significantly improved relative to the substrate, whether through the water immersion test or the oil immersion test.

## 2.7 Corrosion resistance test

After the surface of each test piece and the base material was polished and polished, the cladding layer of each test piece and the upper surface of the substrate were selected as corrosion resistance test faces, and the other surfaces of the test block were wrapped with epoxy resin. It was immersed in 12% HCl solution for two days. After two days, the test block was taken out, and the test block was cleaned with a high-purity water, and then placed in a drying oven to be dried, and the mass was weighed. The corrosion rate was calculated by using Equation 2, and the results are shown in Table 5.

$$v_{\text{corrosion}} = \frac{m_{\text{pre}} - m_{\text{post}}}{St} \quad (2)$$

Where: mpre is the mass of the test block before corrosion, mg; mpost is the mass of the test block after corrosion, mg; S is the area of the corrosion surface of the test block, mm2; t is the corrosion time, which is 2 days.

| Test block number | Weight loss quality $\Delta m$ （mg） | Cladding top surface area S（$mm^2$） | Corrosion rate $v_{corrosion}$ ($mg/mm^2 \cdot day$) |
|---|---|---|---|
| Test block 1 | 0.086 | 189.6790 | 0.000227 |
| Test block 2 | 0.085 | 187.4544 | 0.000227 |
| Test block 3 | 0.086 | 190.6414 | 0.000226 |
| Test block 4 | 0.083 | 182.5901 | 0.000227 |
| Test block 5 | 0.086 | 191.9988 | 0.000224 |
| Test block 6 | 0.084 | 187.6068 | 0.000224 |
| Test block 7 | 0.085 | 188.7872 | 0.000225 |
| Test block 8 | 0.084 | 187.2225 | 0.000224 |
| Test block 9 | 0.085 | 189.7632 | 0.000224 |
| Matrix Test block | 0.228 | 187.1408 | 0.000609 |

Table 5. Corrosion rate of test piece cladding layer obtained under matrix and different process parameters

It can be seen from the data in Table 8 that the corrosion resistance of the test piece cladding layer obtained under different process parameters is improved compared with the matrix. One of the reasons for the analysis is that the microstructure of the cladding layer plays an active role in improving the corrosion resistance. Secondly, the corrosion resistance of the Co element is strong, and at the same time, the Cr, B and Si in the cladding layer are also very resistant. Corrosive. Therefore, the corrosion resistance of the cladding layer is significantly better than that of the substrate.

# 3. Fuzzy comprehensive evaluation

## 3.1 Using improved fuzzy comprehensive evaluation theory

Surface quality and interface characteristics, microhardness, wear resistance, oxidation resistance, compactness and properties of the cladding layer obtained by coating the Co-based alloy powder with different WC particle content on the surface of 1Cr18Ni9Ti stainless steel substrate by improved fuzzy comprehensive evaluation. The analytical data of the six indicators of corrosion resistance were comprehensively evaluated. The main method is to obtain the fuzzy evaluation matrix through the comment collection of each sample factor set. After the expert knowledge and experience, the weight judgment matrix of each evaluation index is obtained, and then the analytic hierarchy method is used to analyze the consistency index of the weight. Find the objective weight coefficient of each evaluation index. Finally, the fuzzy operator is used to evaluate the fuzzy comprehensive evaluation.

### 3.1.1 Subordinate evaluation of cladding quality and interface characteristics

In the comprehensive evaluation of the quality of the cladding layer and the interface characteristics, the CR value is determined based on the actual situation of the surface quality requirements. Because there are no cracks and pores in the macroscopic and microscopic aspects of each block, the combination of the cladding layer and the matrix is good. Therefore, three effects of formation, oxidation and splash are determined without considering the effects of pores, cracks and interface characteristics. The judgment matrix of the aspect is:

$$P_1 = \begin{array}{c} \text{Forming Oxidation Splash} \\ \left[\begin{array}{ccc} 1 & 4 & 5 \\ \frac{1}{4} & 1 & 2 \\ \frac{1}{5} & \frac{1}{2} & 1 \end{array}\right] \end{array} \begin{array}{l} \\ \text{Forming} \\ \text{Oxidation} \\ \text{Splash} \end{array}$$

Get:

$$\lambda_{\max} = 3.0241;$$

$$V = \begin{bmatrix} 0.9471 & 0.2769 & 0.1620 \end{bmatrix}^T;$$

Improved normalization of feature vectors using European metrics:

$$W_1 = \begin{bmatrix} 0.9471 & 0.2769 & 0.1620 \end{bmatrix}^T;$$

$$PW_1 = \begin{bmatrix} 2.8647 & 0.8377 & 0.4899 \end{bmatrix}^T;$$

$$CI_1 = 0.0121; \quad RI_1 = 0.58;$$

$$CR_1 = 0.0209 \le 0.10$$

It can be seen that the above judgment matrix has satisfactory consistency, so the weight coefficient of the comprehensive evaluation of the surface quality is:

$$W_1 = \begin{bmatrix} 0.9471 & 0.2769 & 0.1620 \end{bmatrix}^T$$

On the basis of the surface quality, according to the surface quality subordination comparison table of the literature 14[14], the surface quality subordination fuzzy matrix of samples 1 to 9 is obtained:

$$R_1 = \begin{bmatrix} 0.9 & 0.1 & 0 & 0 & 0 \\ 0.4 & 0.6 & 0 & 0 & 0 \\ 0.4 & 0.6 & 0 & 0 & 0 \end{bmatrix}; \quad R_2 = \begin{bmatrix} 0.7 & 0.3 & 0 & 0 & 0 \\ 0.4 & 0.6 & 0 & 0 & 0 \\ 0.4 & 0.6 & 0 & 0 & 0 \end{bmatrix};$$

$$R_3 = \begin{bmatrix} 0 & 0 & 0.7 & 0.3 & 0 \\ 0 & 0 & 0 & 0.1 & 0.9 \\ 0.4 & 0.6 & 0 & 0 & 0 \end{bmatrix}; \quad R_4 = \begin{bmatrix} 0 & 0 & 0.7 & 0.3 & 0 \\ 0 & 0 & 0 & 0.1 & 0.9 \\ 0 & 0.3 & 0.7 & 0 & 0 \end{bmatrix}; \quad R_5 = \begin{bmatrix} 0.9 & 0.1 & 0 & 0 & 0 \\ 0.4 & 0.6 & 0 & 0 & 0 \\ 0.4 & 0.6 & 0 & 0 & 0 \end{bmatrix};$$

$$R_6 = \begin{bmatrix} 0.9 & 0.1 & 0 & 0 & 0 \\ 0.4 & 0.6 & 0 & 0 & 0 \\ 0 & 0.3 & 0.7 & 0 & 0 \end{bmatrix};$$

$$R_7 = \begin{bmatrix} 0.9 & 0.1 & 0 & 0 & 0 \\ 0.4 & 0.6 & 0 & 0 & 0 \\ 0.4 & 0.6 & 0 & 0 & 0 \end{bmatrix}; \quad R_8 = \begin{bmatrix} 0.7 & 0.3 & 0 & 0 & 0 \\ 0 & 0 & 0 & 0.1 & 0.9 \\ 0.4 & 0.6 & 0 & 0 & 0 \end{bmatrix};$$

$$R_9 = \begin{bmatrix} 0.9 & 0.1 & 0 & 0 & 0 \\ 0.4 & 0.6 & 0 & 0 & 0 \\ 0.4 & 0.6 & 0 & 0 & 0 \end{bmatrix}$$

According to the theory of fuzzy evaluation, the surface quality is evaluated first, and the result should be synthesized by the weight distribution coefficient matrix and the fuzzy matrix $A_1 = W_1^T = \begin{bmatrix} 0.9471 & 0.2769 & 0.1620 \end{bmatrix}$. Among them, respectively, the fuzzy operator is used to perform the compound operation on the matrix, and then the European after normalization under the metric, you get $B_1^* \sim B_9^*$:

$$B_1^* = \begin{bmatrix} 0.9444 & 0.3289 & 0 & 0 & 0 \end{bmatrix};$$

$$B_2^* = \begin{bmatrix} 0.8373 & 0.5467 & 0 & 0 & 0 \end{bmatrix};$$

$$B_3^* = [0.0828 \quad 0.1242 \quad 0.8471 \quad 0.3984 \quad 0.3184]$$
$$B_4^* = [0 \quad 0.0556 \quad 0.8880 \quad 0.3566 \quad 0.2850];$$
$$B_5^* = [0.9444 \quad 0.3289 \quad 0 \quad 0 \quad 0];$$
$$B_6^8 = [0.9461 \quad 0.3040 \quad 0.1114 \quad 0 \quad 0];$$
$$B_7^* = [0.9444 \quad 0.3289 \quad 0 \quad 0 \quad 0];$$
$$B_8^* = [0.8472 \quad 0.4439 \quad 0 \quad 0.0322 \quad 0.2901];$$
$$B_9^* = [0.9444 \quad 0.3289 \quad 0 \quad 0 \quad 0]$$

### 3.1.2 Subordination of hardness

Since the hardness index is already quantified, the fuzzy index is used to determine the membership relationship. Among them, the maximum and minimum hardness HV values are divided into 4 intervals by the equal difference method, wherein the highest hardness is 1 for the good membership degree and 0 for the difference; the lowest hardness is 0 for the good membership degree. The degree is 1, and the membership function of each interval is determined by a semi-trapezoidal, triangular, and semi-trapezoidal distribution. The membership evaluation function is shown in Table 6:

| Fuzzy evaluation | Membership function | HV range |
|---|---|---|
| Good | 1 | HV≥1498.4 |
| | $(x-1265.29)/233.11$ | 1498.4＞HV≥1265.29 |
| | 0 | HV＜1265.29 |
| Better | 0 | HV≥1498.4 |
| | $1-(x-1265.29)/233.11$ | 1498.4＞HV≥1265.29 |
| | $(x-1032.18)/233.11$ | 1265.29＞HV≥1032.18 |
| | 0 | HV＜1032.18 |
| Average | 0 | HV≥1265.29 |
| | $1-(x-1032.18)/233.11$ | 1265.29＞HV≥1032.18 |
| | $(x-799.07)/233.11$ | 1032.18＞HV≥799.07 |
| | 0 | HV＜799.07 |
| Poor | 0 | HV≥1032.18 |
| | $1-(x-799.07)/233.11$ | 1032.18＞HV≥799.07 |
| | $(x-565.96)/233.11$ | 799.07＞HV≥565.96 |
| | 0 | HV＜565.96 |
| Difference | 0 | HV≥799.07 |
| | $1-(x-565.96)/233.11$ | 799.07＞HV≥565.96 |
| | 1 | HV＜565.96 |

Table 6. Hardness index versus membership function comparison table

Since the hardness index of the cladding layer is related to the membership function, the hardness value needs to be the hardness value of the cladding layer. We take the hardness values of the first three measurement points of each test block for arithmetic averaging, then perform fuzzy evaluation on the hardness value of each sample cladding layer according to the above membership function, and then normalize the process with European metrics to obtain $C_1^* \sim C_9^*$:

$$C_1^* = [0 \quad 0.2559 \quad 0.9667 \quad 0 \quad 0];$$
$$C_2^* = [0 \quad 0 \quad 0.9996 \quad 0.0279 \quad 0];$$
$$C_3^* = [0.2583 \quad 0.9661 \quad 0 \quad 0 \quad 0];$$
$$C_4^* = [0 \quad 0 \quad 0.9951 \quad 0.0994 \quad 0];$$
$$C_5^* = [0 \quad 0 \quad 0 \quad 0.1986 \quad 0.9801];$$
$$C_6^* = [0 \quad 0 \quad 0.8900 \quad 0.4560 \quad 0];$$
$$C_7^* = [0 \quad 0 \quad 0 \quad 0.9263 \quad 0.3769];$$
$$C_8^* = [0 \quad 0 \quad 0.1229 \quad 0.9924 \quad 0];$$
$$C_9^* = [0 \quad 0 \quad 0.4696 \quad 0.8829 \quad 0];$$

### 3.1.3 Subordination of wear performance

The subordination method of wear performance is the same as the hardness index. The maximum and minimum friction coefficient values are divided into 4 sections by the equal difference method, but the hardness index is just the opposite. Similarly, the anti-wear performance of each sample cladding layer was evaluated based on the membership function. Then, after normalization with the European metric, you get $D_1^* \sim D_9^*$:

$$D_1^* = [0 \quad 0 \quad 0 \quad 0.9644 \quad 0.2646];$$
$$D_2^* = [0 \quad 0 \quad 0 \quad 0.8396 \quad 0.5432];$$
$$D_3^* = [0 \quad 0 \quad 0.1962 \quad 0.9806 \quad 0];$$
$$D_4^* = [0 \quad 0 \quad 0 \quad 0.0010 \quad 1]$$
$$D_5^* = [0.3076 \quad 0.9515 \quad 0 \quad 0 \quad 0];$$
$$D_6^* = [0.4157 \quad 0.9095 \quad 0 \quad 0 \quad 0];$$
$$D_7^* = [1 \quad 0 \quad 0 \quad 0 \quad 0];$$
$$D_8^* = [0 \quad 0.5250 \quad 0.8511 \quad 0 \quad 0];$$
$$D_9^* = [0 \quad 0.1007 \quad 0.9949 \quad 0 \quad 0];$$

### 3.1.4 Subordinate evaluation of antioxidant performance

The evaluation method of antioxidant performance is the same as the wear performance index. Similarly, the oxidation resistance of each sample cladding layer is fuzzy evaluated according to the membership function. Then, after normalization with the European metric, you get $E_1^* \sim E_9^*$:

$$E_1^* = [0 \quad 0 \quad 0 \quad 0.2631 \quad 0.9648];$$
$$E_2^* = [0 \quad 0 \quad 0 \quad 0.6369 \quad 0.7709];$$
$$E_3^* = [0 \quad 0 \quad 0 \quad 0.7399 \quad 0.6727];$$
$$E_4^* = [0 \quad 0 \quad 0 \quad 0.0499 \quad 0.9988];$$
$$E_5^* = [0 \quad 0.4090 \quad 0.9125 \quad 0 \quad 0];$$

$$E_6^* = [0 \quad 0.8516 \quad 0.5242 \quad 0 \quad 0];$$

$$E_7^* = [1 \quad 0 \quad 0 \quad 0 \quad 0];$$

$$E_8^* = [0 \quad 0 \quad 0.8269 \quad 0.5624 \quad 0];$$

$$E_9^* = [0 \quad 0 \quad 0.1962 \quad 0.9806 \quad 0];$$

### 3.1.5 Substitute judgment of compactness

The substitute evaluation method of compactness is the same as the wear performance index. The compactness is evaluated as an indicator, so we must take into account the weight gain of the water immersion and oil immersion of each test block. Therefore, we use the average of the two weight gains to judge the degree of membership. Similarly, the compactness of each sample cladding layer was evaluated based on the membership function. Then, after normalization using the European metric, $F_1^* \sim F_9^*$:

$$F_1^* = [0 \quad 0.1095 \quad 0.9940 \quad 0 \quad 0];$$

$$F_2^* = [0 \quad 0.9969 \quad 0.0784 \quad 0 \quad 0];$$

$$F_3^* = [0 \quad 0.8189 \quad 0.5740 \quad 0 \quad 0];$$

$$F_4^* = [0 \quad 0 \quad 0 \quad 0.5095 \quad 0.8605];$$

$$F_5^* = [0 \quad 0.9342 \quad 0.3568 \quad 0 \quad 0];$$

$$F_6^* = [0 \quad 0 \quad 0.8075 \quad 0.5898 \quad 0];$$

$$F_7^* = [0.7836 \quad 0.6212 \quad 0 \quad 0 \quad 0];$$

$$F_8^* = [0.2954 \quad 0.9554 \quad 0 \quad 0 \quad 0];$$

$$F_9^* = [0.9964 \quad 0.0847 \quad 0 \quad 0 \quad 0];$$

### 3.1.6 Subordination of corrosion resistance

The evaluation method of corrosion resistance is the same as the wear performance index. Similarly, the corrosion resistance of each sample cladding layer is fuzzy evaluated according to the membership function. Then, after normalization using the European metric, $G_1^* \sim G_9^*$:

$$G_1^* = [0 \quad 0 \quad 0 \quad 0.3162 \quad 0.9487];$$

$$G_2^* = [0 \quad 0 \quad 0 \quad 0.3162 \quad 0.9487];$$

$$G_3^* = [0 \quad 0 \quad 0.7071 \quad 0.7071 \quad 0];$$

$$G_4^* = [0 \quad 0 \quad 0 \quad 0.3162 \quad 0.9487];$$

$$G_5^* = [1 \quad 0 \quad 0 \quad 0 \quad 0];$$

$$G_6^* = [1 \quad 0 \quad 0 \quad 0 \quad 0];$$

$$G_7^* = [0 \quad 0.9487 \quad 0.3162 \quad 0 \quad 0];$$

$$G_8^* = [1 \quad 0 \quad 0 \quad 0 \quad 0];$$

$$G_9^* = [1 \quad 0 \quad 0 \quad 0 \quad 0];$$

### 3.2 Fuzzy comprehensive evaluation

#### 3.2.1 Cladding performance comprehensive weight coefficient

Because the valve sealing surface is prone to corrosion failure and wear failure under high temperature and high pressure conditions, corrosion resistance and wear resistance are more important than other performances, so this performance score is higher than other performances. Minute. In addition, easy oxidation will also cause certain corrosion, hardness will also affect the wear resistance, so the material's oxidation resistance and hardness are important between corrosion resistance and wear resistance and other properties, Also between, give 3 points. Then determine the judgment matrix of the comprehensive evaluation of the cladding test block:

Surface Hardness Abrasion Anti-oxidation Compactness Preservation

$$P_2 = \begin{bmatrix} 1 & 2 & 2 & 3 & 2 & 3 \\ 1/2 & 1 & 1 & 3 & 1 & 3 \\ 1/2 & 1 & 1 & 2 & 1 & 2 \\ 1/3 & 1/3 & 1/2 & 1 & 1 & 1 \\ 1/2 & 1 & 1 & 1 & 1 & 2 \\ 1/3 & 1/3 & 1/2 & 1 & 1/2 & 1 \end{bmatrix} \begin{matrix} \text{Surface} \\ \text{Hardness} \\ \text{Abrasion} \\ \text{Anti-oxidation} \\ \text{Compactness} \\ \text{Preservation} \end{matrix}$$

Obtain:

$$\lambda_{\max} = 6.1140;$$

$$V = \begin{bmatrix} 0.6855 & 0.4403 & 0.3753 & 0.2128 & 0.3405 & 0.1850 \end{bmatrix}^T;$$

Improved normalization of feature vectors using European metrics:

$$W_2 = \begin{bmatrix} 0.6855 & 0.4403 & 0.3753 & 0.2128 & 0.3405 & 0.1850 \end{bmatrix}^T;$$

$$PW_2 = \begin{bmatrix} 4.1911 & 2.6922 & 2.2944 & 1.3012 & 2.0817 & 0.1310 \end{bmatrix}^T;$$

$$CI_1 = 0.0228; \quad RI_1 = 1.24;$$

$$CR_1 = 0.0184 \le 0.10.$$

It can be seen that the above judgment matrix has satisfactory consistency, so the weight coefficient of the comprehensive evaluation of the surface quality is:

$$W_2 = \begin{bmatrix} 0.6855 & 0.4403 & 0.3753 & 0.2128 & 0.3405 & 0.1850 \end{bmatrix}^T$$

#### 3.2.2 Comprehensive evaluation of cladding properties

Fuzzy comprehensive evaluation of the factor set: {surface quality, microhardness, wear performance, oxidation resistance, compactness, corrosion resistance}, comment collection: {good, better, average, poor, poor}. From the surface quality evaluation, microhardness evaluation, wear performance evaluation, antioxidant performance evaluation, compactness evaluation and corrosion resistance evaluation, the fuzzy matrix of each test block was obtained. The first row of the matrix takes the value, the second row takes the value, the third row takes the value, the fourth row takes the value, the fifth row takes the value, and the sixth row takes the value. The zadeh operator is used to perform the composite operation on the fuzzy matrix to obtain the evaluation result, and then the normalized processing under the European metric is obtained $I_i^*$ :

$$I_1^*=[0.5116 \quad 0.2967 \quad 0.6038 \quad 0.3765 \quad 0.3794]$$
$$I_2^*=[0.4503 \quad 0.5603 \quad 0.3662 \quad 0.4091 \quad 0.4263]$$
$$I_3^*=[0.1056 \quad 0.4888 \quad 0.6072 \quad 0.5755 \quad 0.2238]$$
$$I_4^*=[0 \quad 0.0222 \quad 0.6099 \quad 0.3095 \quad 0.7292]$$
$$I_5^*=[0.6438 \quad 0.6709 \quad 0.2144 \quad 0.0594 \quad 0.2931]$$
$$I_6^*=[0.6380 \quad 0.4713 \quad 0.5511 \quad 0.2589 \quad 0]$$
$$I_7^*=[0.8931 \quad 0.3641 \quad 0.0348 \quad 0.2425 \quad 0.0987]$$
$$I_8^*=[0.5964 \quad 0.5690 \quad 0.3783 \quad 0.3984 \quad 0.1369]$$
$$I_9^*=[0.7896 \quad 0.1969 \quad 0.4191 \quad 0.4026 \quad 0]$$

Give the comment collection: {good, better, average, poor} give the weight of {3, 2, 1, -1, -2} respectively, and the comprehensive result of the test block No. 6 can be obtained optimally.

Therefore, the best cladding layer obtained by the laser cladding test of the valve sealing surface after the fuzzy comprehensive evaluation is the No. 7 test block. The optimal test process parameters are: laser power P is 1.1 kW, and scanning speed Vb is 800 mm/ Min, the powder feeding rate Vf is 20%, and the WC content is 20% by weight.

# 4. Summary

In order to obtain the performance of the cladding layer for laser repair and remanufacturing of the valve sealing surface, the laser cladding test of 1Cr18Ni9Ti stainless steel with high temperature and high pressure valve sealing surface is carried out, and the laser power P and powder feeding during the laser cladding process are adjusted. Three important process parameters, rate Vf and scanning speed Vb, and WC particles with different ratios in Co-based alloy powders, the cladding layers under different process parameters are obtained, according to the properties of the cladding layer and the matrix test block. Test, get the following conclusions:

(1) Visual examination of the macroscopic features showed that all the test pieces had no pores and cracks; microscopically, the interface characteristics of the cladding layer and the matrix material of each test block are observed, and it was found that all the test piece cladding layer and the matrix are combined. WC distribution is relatively uniform, there is no obvious sinking phenomenon, and after laser beam heating treatment, WC particles still maintain their original spherical appearance, only a slight dissolution at the edge, indicating WC particles and Ni-based alloy The same is also for metallurgical bonding.

(2) Through the microhardness test of each cladding layer, it is found that the hardness value of the cladding layer is 2.3~5 times higher than that of the substrate. The hardness of the cladding layer to which the WC particles are added fluctuates greatly, and the WC particles are added as a hard phase to the Ni-based alloy powder to refine the crystal grains and improve the hardness.

(3) Through the dry friction test, the oxidation resistance test, the tightness test and the corrosion resistance test of each cladding layer test block and the base test block, it is found that no matter which process is obtained, the cladding is obtained. The layers are all significantly improved compared to the matrix material.

(4) Finally, the fuzzy comprehensive evaluation under the improved European metric weight coefficient is used to comprehensively evaluate the analysis data of the laser cladding layer, and the optimal process parameters for the repair of the high temperature and high pressure valve sealing surface and the addition ratio of WC powder are obtained. The laser power P was 1.1 kW, the scanning speed Vb was 800 mm/min, the powder feeding rate Vf was 20%, and the WC content was 20% by weight.

# 5. Acknowledgements

This work was financially supported by Xinjiang uygur autonomous region high-tech research and development

project (201513102) and Xinjiang uygur autonomous region youth natural science fund project (2017D01C062).

# References

1. Shi Shihong, Wang Xinlin. Experimental study on sealing surface of laser cladding chemical valve[J]. Laser Technology. 1998; 22(6): 60-60.
2. Liu Shuang, Liu Xiubo, Fu Geyan, *et al*. Laser Cladding Technology and Its Research Progress in Nuclear Power Valves[J]. Material Guide. 2009; 23(s1):203-205.
3. Lin Jinguo, Zeng Xiaolin, Tong Xiaochuan, *et al*. Numerical Simulation of Flow Characteristics of Large High Pressure Steam Valves[J]. Fluid Machinery. 2015; (2):56-59.
4. Cai Dingshuo, Tao Zhengliang, Yan Chunlei. Qualitative Analysis of Airflow Characteristics in High Pressure Steam Valves[J]. Turbine Technology. 2003; 45(1): 36-38.
5. Du Chunhua. Repair of 103-JT Main Steam Valve by Synthetic Synthesis[J]. Chuanhua. 2008(3): 34-35.
6. Tabernero, I. Lamikiz, A. Ukar.E, et a1. Parameter Optimization for Mould and Die Recovering Using Laser Cladding[J]. Third Manufacturing Engineering Society International Conference. 2009:484-493.
7. Dubourg L, St. Georges L. Optimization of Laser Cladding Process Using Taguchi and EM Methods for MMC Coating Production[J]. Journal of Thermal Spray Technology. 2006, 15(4): 790-79.
8. Ge Jiangbo, Zhang Anfeng, Li Dichen, *et al*. Research on laser metal direct forming DZ125L superalloy parts process[J]. China Laser. 2011; 38(7): 119-125.
9. Xiong Wei, Zhang Qingmao, Xia Qi *et al*. Effect of high temperature heat treatment on microstructure and properties of laser cladding alloy layer[J]. Journal of Applied Lasers. 2013; 33(6):233-238.
10. Liu Furong, Gao Qian, Gao Dengpan, *et al*. Analysis of Cracking Behavior of Laser Cladding WC Reinforced Composite Coatings[J]. Journal of Materials Engineering. 2003(5): 37-39.
11. Gu Jiqing. Stainless Steel Application Handbook [M]. Beijing: Chemical Industry Press, 2008.
12. Wen Shizhu, Huang Ping. Principles of Tribology (4th Edition) [M]. Beijing: Tsinghua University Press, 2012.
13. Zhang Yongzhen *et al*. Dry Tribology of Materials (2nd Edition) [M]. Beijing: Science Press, 2012.
14. Ma Yunzhe, Dong Shiyun, Xu Binshi, *et al*. Process optimization of iron-based alloy laser cladding technology [J]. China Surface Engineering. 2006; 19(s1): 154-160.